Quantum cascade driving: Dissipatively mediated coherences

Shahabedin C. Azizabadi,* Nicolas L. Naumann, Manuel Katzer, Andreas Knorr, and Alexander Carmele
Technische Universität Berlin, Institut für Theoretische Physik, Nichtlineare Optik und Quantenelektronik, Hardenbergstraße 36, 10623 Berlin, Germany

(Received 19 June 2017; revised manuscript received 11 July 2017; published 8 August 2017)

Quantum cascaded systems offer the possibility to manipulate a target system with the quantum state of a source system. Here, we study in detail the differences between a direct quantum cascade and coherent or incoherent driving for the case of two coupled cavity-QED systems. We discuss qualitative differences between these excitations scenarios, which are particularly strong for higher-order photon-photon correlations: $g^{(n)}(0)$ with $n > 2$. Quantum cascaded systems show a behavior differing from the idealized cases of individual coherent or incoherent driving and allow one to produce qualitatively different quantum statistics. Furthermore, the quantum cascaded driving exhibits an interesting mixture of quantum coherent and incoherent excitation dynamics. We develop a measure where the two regimes intermix and quantify these differences via experimentally accessible higher-order photon correlations.

DOI: 10.1103/PhysRevA.96.023816

I. INTRODUCTION

Quantum light sources are realized for many different material platforms in semiconductor, atom, and molecular systems [1–5] and offer an exciting testbed for nonlinear quantum dynamics [6], including quantum ghost imaging, two-photon spectroscopy [7–9], and quantum light spectroscopy [10–12]. Prototypical single-photon emitters based on semiconductor nanostructures are produced [13–15] and used in quantum cryptography protocols [16–18] and quantum sensing [19]. Recently, practical realizations of intense and tunable thermal sources have become accessible [20–23] and are applied experimentally for photon-statistics excitation spectroscopy [21,24] and to read-out quantum beating of hyperfine levels via a modulation with pulse separation [20]. Polarization-entangled photon sources [25], another class of quantum light sources, are electrically driven and triggered on demand [26]. For highly efficient and indistinguishable twin photon sources [27] this is possible as well in the context of N-photon bundle emitters [3] and on-demand time-ordered photon pairs [28].

The rich variety of quantum light is accompanied by exciting proposals. Single photon excitation purifies nonclassical states and suppresses fluctuations [29] and allows for Hilbert-state addressing [30]. Entangled photon pairs are proposed for ultrafast double-quantum-coherence spectroscopy of excitons with entangled photons [31] or quantum gates based on entanglement swapping protocols [32]. The Schmidt decomposition allows one to analyze the material response function to obtain information about otherwise inaccessible resonances of a complex system [33]. This connects to the context of quantum optical spectroscopy [11,34] and nonlinearity sensing via photon-statistics excitation spectroscopy [1,22,35,36].

A very convenient method to simulate quantum excitation experiments is the quantum cascade setup developed at the same time by Gardiner [37] and Carmichael [38]. In this context it was shown that certain photon statistics may alter the response of the target system in a cascaded setup [39]. In these previous studies, the focus was on simple sources. Recently, the impacts of the cascaded setup in correlations up to third order were considered for the case where the output of a two-level system is used to drive a cavity [30] and another two-level system [40]. There, it was also suggested to use higher-order correlation functions to better characterize the target light field. In the following, we will consider the Jaynes-Cummings model as a prototype for laser-like sources and quantum light sources. The main target of interest in our study is a Tavis-Cummings model with two emitters in order to observe the impact of a larger nonlinearity in the context of cascaded coupling.

The quantum cascade approach allows a self-consistent mapping of the quantum excitation onto a second system, via the quantum Langevin [37] or quantum stochastic Schrödinger equations [41,42]. The coupling mechanism of the cascaded system is a dissipatively mediated excitation process where the output (measurement) of the source system is the input (excitation) of the target system. This excitation strategy differs strongly from a bath input (thermal equilibrium) or laser excitation, which adds coherence to the system. In contrast, the quantum cascaded driving allows a photon-statistical fine tuning in between these regimes and renders a transient regime accessible, where thermal statistics and quantum coherences coexist and intertwine via quantum emitters. The cascaded coupling does not consider back-action and ignores time delays between the source and target systems. Systems incorporating these effects are more difficult to model from a theoretical perspective; however, the new degrees of freedom are an alternative way to control the photon statistical output of a system [43].

In this work, we theoretically discuss this intermixing and transition dynamics by employing a quantum cascaded system. This kind of quantum cascaded setup may be realized experimentally by implementing the microcavity containing the emitters inside a waveguide. To ensure the unidirectionality of the coupling mechanism, topological photonics structures can be exploited [44], where light is only able to propagates into one direction. In Sec. II, we derive the basic quantum cascaded coupling in the master equation formalism, equivalent to the method of Langevin operators [30,45] and the quantum stochastic Schrödinger equation [38,46]. We apply this

*shahab@ut.ee

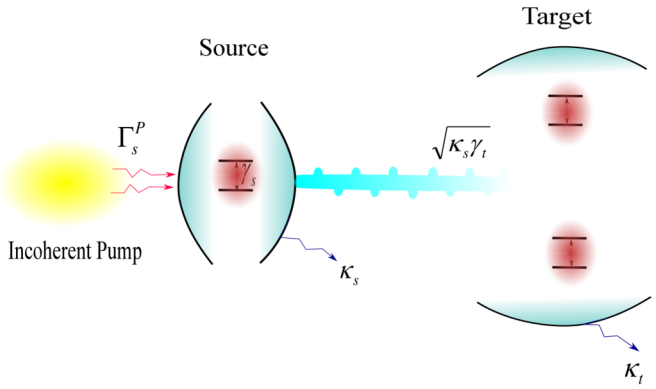

FIG. 1. Schematic depiction of the studied setup. The source cavity, which contains a TLS, is pumped incoherently with rate Γ_s^P. The emission of the source cavity is fed into the one or two emitters contained in the target cavity.

quantum cascaded coupling in Sec. III to a specific example: an incoherently pumped single quantum emitter in a cavity as the source and as the target one or two identical quantum emitters coupled to a cavity. The intensity-intensity correlation $g^{(2)}(0)$ of the target system follows the intensity-intensity correlation in a degraded fashion, which is expected for cascaded cavities with nonlinearities [47]. In Sec. IV, however, we show that the response of the target system follows not universally the output of the source system: Higher-order intensity correlations $g^{(n)}(0)$ exhibit a completely different picture. Via these higher-order correlations, we finally discuss the qualitatively different behavior of the cascaded setup in comparison to the typical excitation scenarios of coherent and incoherent pumping in Sec. V. In Sec VI, we conclude and summarize the findings.

II. QUANTUM CASCADE MODEL

To investigate the dynamics of a quantum cascaded system, we derive a master equation in the Born-Markov limit using a thermal bath [30,45,48]. Employing these approximations allows us to trace out the bath degrees of freedom and derive a master equation for this system, which still is numerically expensive, but tractable. To allow for more complex bath states, more expensive models would be needed [49–51], which take into account the bath itself, e.g., [52]. In the model employed here with a second-order Born and Markov approximation, more complicated types of reservoirs cannot be treated.

The assumption of a thermal bath will lead to a coupling mechanism, which imprints the intrinsic incoherence of the bath partially onto the target while still preserving some of the properties of the source statistics.

We will consider systems as depicted in Fig. 1, i.e., a source quantum system with Hamiltonian H_s coupled via a thermal bath H_c to target quantum system H_t. The full Hamiltonian reads $H = H_0 + H_s + H_c + H_t$, with H_0 including the free evolution dynamics of all quantities in the total system. At this point, we do not define H_s and H_t, but focus on the coupling Hamiltonian H_c, which is given in a rotating frame in correspondence to H_0 and reads in the rotating wave approximation

$$\frac{H_c}{\hbar} = \int d\omega\, b(\omega)\left[K_\omega^s J_s^\dagger(t) + K_\omega^t J^\dagger(t,\tau)\right] + \text{H.c.}, \qquad (1)$$

where τ describes the finite time delay between the target and source system and J_s, J_t describe a single operator or a superposition in the source and target system, respectively. The coupling of the source/target system to the connecting reservoir is $K_\omega^{s/t}$, which we set independently of the frequency in the narrow bandwidth limit $K_\omega^{s/t} \equiv K_0^{s/t}$.

To derive the quantum cascaded coupling, we employ the canonical derivation of the master equation in the Born-Markov limit with $\chi_{\text{tot}}(t) = \rho(t)\rho_B(0)$, assuming the coupling reservoir is in equilibrium and in a thermal state [53,54]:

$$\left.\frac{d\rho}{dt}\right|_c = -\frac{1}{\hbar^2}\int_0^t ds\, \text{Tr}_B\{[H_c(t),[H_c(s),\rho(t)\rho_B]]\}. \qquad (2)$$

We assume the thermal bath to be in the vacuum state and consider only contributions proportional to $\langle b(\omega)b^\dagger(\omega)\rangle$ and assume the commutator relations $[b(\omega),b^\dagger(\omega')] = \delta(\omega-\omega')$. Given these conditions, the double commutator can be evaluated, and we get the following master equation after tracing out the bath degrees of freedom:

$$\begin{aligned}\left.\frac{d\rho}{dt}\right|_c =& -2\pi\sum_{i=s,t}(K_0^i)^2\int_0^t ds\,\delta(s-t)[J_i^\dagger(t)J_i(s)\rho(s) - J_i(t)\rho(s)J_i^\dagger(s) - J_i(s)\rho(s)J_i^\dagger(s) + \rho(s)J_i^\dagger(s)J_i(t)]\\ &- 2\pi K_0^s K_0^t\int_0^t ds\,\delta(s-(t-\tau))[J_t^\dagger(t)J_s(s)\rho(s) - J_t(t)\rho(s)J_s^\dagger(s) - J_s(s)\rho(s)J_t^\dagger(t) + \rho(s)J_s^\dagger(s)J_t(t)]\\ &- 2\pi K_0^s K_0^t\int_0^t ds\,\delta(s-(t+\tau))[J_s^\dagger(t)J_t(s)\rho(s) - J_s(t)\rho(s)J_t^\dagger(s) - J_t(s)\rho(s)J_s^\dagger(s) + \rho(s)J_t^\dagger(s)J_s(t)]. \qquad (3)\end{aligned}$$

We take into account that $\int_0^t ds\,\delta(t-s)h(s) = h(t)/2$ and that $s \leqslant t$. By definition $K_0^i = \sqrt{\gamma_i/(2\pi)}$, where γ_i are the decay rates of the subsystems that couple source and target. Then, one coupling contribution between target and source vanishes. The full master equation in the Born-Markov limit reads

$$\begin{aligned}\frac{d\rho}{dt} =& \frac{1}{i\hbar}[H_s + H_t,\rho] + \sum_{i=s,t}\frac{\gamma_i}{2}(2J_i(t)\rho(t)J_i^\dagger(t) - \{J_i^\dagger(t)J_i(t),\rho(t)\})\\ &- \sqrt{\gamma_s\gamma_t}(J_t^\dagger(t)J_s(t_D)\rho(t_D) - J_t(t)\rho(t_D)J_s^\dagger(t_D)) - \sqrt{\gamma_s\gamma_t}(\rho(t_D)J_s^\dagger(t_D)J_t(t) - J_s(t_D)\rho(t_D)J_t^\dagger(t)), \qquad (4)\end{aligned}$$

with $t_D = t - \tau$. In our setup, the delay τ is small and can be set to zero safely within our Markovian approximation. Transforming back from the rotating frame, the full master equation reads

$$\frac{d\rho}{dt} = \frac{1}{i\hbar}[H_0 + H_s + H_t, \rho] + \sum_{i=s,t} \frac{\gamma_i}{2}(2J_i\,\rho J_i^\dagger - \{J_i^\dagger J_i\,, \rho\}) - \sqrt{\gamma_s\gamma_t}([J_t^\dagger, J_s\,\rho] + [\rho J_s^\dagger, J_t\,]). \quad (5)$$

Given this result, we can investigate different kinds of systems and study the particular features of a quantum cascaded driving. To characterize the cascaded driving, we choose first a specific system and then propose the photon-photon correlation functions as a measure for coherence in the system. We will see that the cascaded system exhibits different regimes of excitation depending on the source excitation; however, the source state is not straightforwardly mapped to the target system. Remarkably, it still shows traits of a coherent driving setup, although the cascaded driving is of purely dissipative nature.

III. EXAMPLE: COUPLED CQED SYSTEMS

As a platform to investigate quantum excitation in comparison to coherent and incoherent driving, we focus on a coupled cavity quantum electrodynamics (CQED) system, Fig. 1. As a source system, we consider a single emitter coupled to a single cavity mode, which is the prototypical Jaynes-Cummings Hamiltonian:

$$H_s = \hbar g_s(a_s^\dagger \sigma_s^- + \sigma_s^+ a_s), \quad (6)$$

where $g_s = 0.1$ ps^{-1} denotes the coupling element between the cavity field with creation (annihilation) operators $a^{(\dagger)}$ and the fermionic degrees of freedom described via the spin Pauli matrices $\sigma_s^{(+/-)}$. The coupling operator from the source to the cavity is chosen to be $J_s := a_s$. To control the source system, we assume an incoherent pumping mechanism. For far-off resonant driving, this pump mechanism can safely be described via [55]

$$\mathcal{D}\big[\sqrt{\Gamma_s^P}\sigma_s^+\big]\rho := \Gamma_s^P(2\sigma_s^+\rho\sigma_s^- - \{\sigma_s^-\sigma_s^+, \rho\}), \quad (7)$$

assuming the transfer of excitation from the ground state to the excited state of the fermionic system, and the definition $\mathcal{D}[J]\rho := 2J\rho J^\dagger - \{J^\dagger J, \rho\}$. In the following, we will fix all parameters (cf. Table I) but Γ_s^P, which is controllable via the intensity of the applied external pumping field, or even electrically steerable in semiconductor nanotechnology platforms [1,56–58].

The source is an incoherently pumped single emitter coupled to a single cavity mode. Depending on the pumping strength, the statistics of the output field can be tuned over a wide regime; starting with weak pumping in the single-photon, or antibunching regime $g^{(2)}(0) = \langle (a_s^\dagger)^2 (a_s)^2\rangle / \langle a_s^\dagger a_s\rangle^2 < 1$, the idealized two-level system (TLS) may be brought to the thermal state for a pumping parameter $\Gamma_s^P \gg g_s$. This may not be true for more complex quantum systems such as semiconductor quantum dots, where energetically higher lying multiexciton states may be excited. This is beyond the scope of this work, but may be interesting for future studies as realistic quantum dots imprint distinctive signatures on the output of a possibly more realistic light source [23].

TABLE I. Parameters used for the cascaded setup throughout the paper.

Parameter	Value (ps^{-1})
g_s	0.1
g_t	0.1
γ_s	0.02
γ_t	0.5
κ_s	0.1
κ_t	0.005

To complete the picture, we assume a radiative decay for the source via

$$\mathcal{D}[\sqrt{\gamma_s}\sigma_s^-]\rho := \Gamma_r^s(2\sigma_s^-\rho\sigma_s^+ - \{\sigma_s^+\sigma_s^-, \rho\}). \quad (8)$$

The radiative decay amounts to $\Gamma_r^s = 0.02$ ps^{-1}. So, we do not assume perfect $\beta = 1$ laser dynamics for the single emitter laser, as radiative decay is not fully absorbed by the cavity mode [59].

As a target system, we choose the Tavis-Cummings Hamiltonian with two emitters:

$$H_t = \hbar \sum_{j=1,2} g_{j,t}(a_t^\dagger \sigma_{j,t}^- + \sigma_{j,t}^+ a_t), \quad (9)$$

where the emitter of the target system $\sigma_{j,t}^{-/+}$ couples to the single mode cavity with the strength $g_{j,t} = g_t = 0.1$ ps^{-1} and the emitters are identical. Here, the coupling operator from the target system is chosen to be $J_{i,t} := \sigma_{i,t}^-$ ($i = 1,2$); i.e., the coupling to the source is individual and not in superposition. We assume an additional cavity loss for the target system via

$$\mathcal{D}[\sqrt{\kappa_t}a_t]\rho := \kappa_t(2a_t\,\rho a_t^\dagger - \{a_t^\dagger a_t\,, \rho\}) \quad (10)$$

and setting the photon lifetime $\kappa_t = 0.005$ ps^{-1}.

The free evolution is governed by H_0 and given as

$$H_0 = \hbar\omega_0 \sum_{i=s,t} a_i^\dagger a_i + \hbar\omega_e\left(\sigma_s^+\sigma_s^- + \sum_{i=1,2}\sigma_{t,i}^+\sigma_{t,i}^-\right), \quad (11)$$

We assume a resonant dynamics between the cavity and the emitter $\omega_e = \omega_0$ and also in between the source and target. Therefore, the full master equation reads

$$\frac{d\rho}{dt} = \frac{1}{i\hbar}[H_0 + H_s + H_t, \rho] + \mathcal{D}\big[\sqrt{\Gamma_s^P}\sigma_s^+\big]\rho + \mathcal{D}[\sqrt{\gamma_s}\sigma_s^-]\rho + \mathcal{D}[\sqrt{\kappa_s}a_s]\rho + \mathcal{D}[\sqrt{\kappa_t}a_t\,]\rho + \sum_{i=1,2}\mathcal{D}[\sqrt{\gamma_t}\sigma_{t,i}^-]\rho - \sqrt{\kappa_s\gamma_t}\sum_{i=1,2}([\sigma_{t,i}^+, a_s\,\rho] + [\rho a_s^\dagger, \sigma_{t,i}]). \quad (12)$$

This master equation is numerically evaluated with a fourth-order Runge-Kutta algorithm for different values of Γ_s^P. We keep throughout the discussion all other values

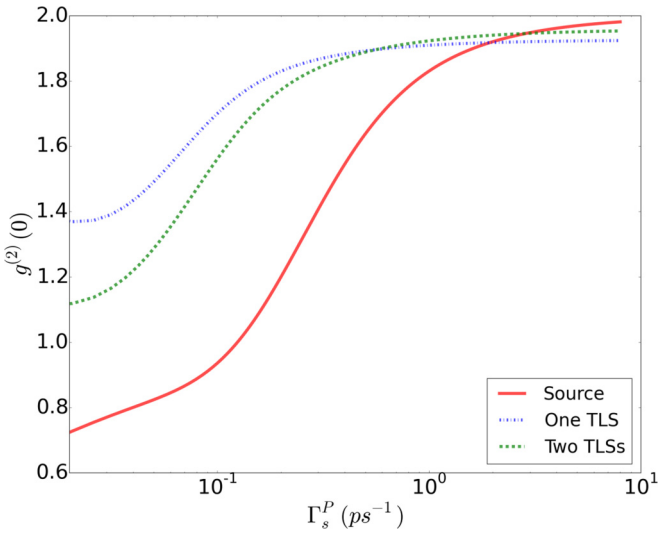

FIG. 2. Second-order correlation functions $g^{(2)}(0)$ of source (red, solid) and one (blue, dashed dotted) and two (green, dashed) tLSs in the target cavity. For low pump rates the target, in contrast to the source, shows rather a bunching behavior. When increasing the pump strength, for both source and target, a transition to the thermal regime occurs.

fixed and cast the master equation (12) into the basis $\langle e_s, p_s, e_t, p_t|\rho|e_s', p_s', e_t', p_t'\rangle$ with e_i emitter states and p_i photon manifolds of source and target $i = s,t$. We compute the observables for different photon manifold cutoffs $p_i < N_i$ until convergence is reached; i.e., the corresponding and discussed observable do not change by increasing the cutoff further. We restrict our discussion in the following to observables of photon manifolds $p_i \leqslant 10$.

We discuss the response of the target system with respect to the photonnstatistics of the output field. The output is included via the cavity loss of the target, and can be measured in Hanbury Brown and Twiss setups via the second-order correlation function, defined in the steady state limit as [60]

$$g^{(2)}_{\rm stat}(\tau) = \lim_{t\to\infty} \frac{\langle a_i^\dagger(t) a_i^\dagger(t+\tau) a_i(t+\tau) a_i(t)\rangle}{\langle a_i^\dagger(t) a_i(t)\rangle^2}, \qquad (13)$$

where for the source $i = s$ and for the target cavity $i = t$. We consider here only the coincidence rates for zero delay $\tau = 0$, as in this limit quantum effects in the correlation are prominent.

In Fig. 2, we numerically evaluate $g^{(2)}(0)$ for the source (red, solid) and target with one (blue, dashed dotted) and two (green, dashed) TLSs for different incoherent pumping strengths Γ_s^P.

The source can be driven into the antibunching regime $g^{(2)} < 1$ for driving strengths of $\Gamma_s^P < g_s$, where single photons are emitted. The cavity coupling is not strong enough to produce more than one cavity photon, before the cavity loss and dissipation forces the photon to leave the resonator. The source dynamics stays antibunched for a wide range of parameters and, for even larger pumping $\Gamma_s^P > g_s$, the pumping induced dephasing adiabatically eliminates the emitter dynamics and the output field equilibrates into a thermal state for the chosen electronic system [55, 61,62].

Focusing now on the target dynamics, we observe that the dissipative coupling via the reservoir leads to a more classical response for one (blue, dashed dotted) as well as two TLSs (green, dashed). In comparison to the source statistics, even in the case of two quantum emitters, i.e., with a stronger quantum nonlinearity, the photon statistics in target cavity is less nonclassical. We can explain this due to the dissipative transfer mechanism between the cavities, leading to thermal mixture and loss of coherence from the source to the target. We observe furthermore that, in the regime $\Gamma_s^P > g_s$, the response follows the source dynamics, and we conclude that a quantum cascaded coupling does not qualitatively change the second-order photon correlation function of the target.

However, we will see that this is not the case for higher-order photon correlation functions, which we discuss in the next section.

IV. BEYOND THE SECOND ORDER PHOTON CORRELATION

Experimentally, higher-order photon correlations have become accessible [63]. They allow one to characterize the quantum light field in photon detection experiments more precisely. For example, a $g^{(2)}(0) \approx 1$ is often taken to be a sign for a coherent light field (in the Glauber state), or a Fock state with a large photon number: $g^{(2)}_{\rm Fock}(0) = 1 - 1/N \to 1$ for $N = \langle a^\dagger a\rangle \gg 1$. However, only considering higher-order correlations allows for a definite characterization of the light field. These are defined for $\tau = 0$ and in the steady state as

$$g^{(n)}_{\rm stat}(0) = \frac{\langle a_i^{\dagger n} a_i^{\ n}\rangle}{\langle a_i^\dagger a_i\rangle^n}, \qquad (14)$$

where $i = s$ for the source and $i = t$ for the target cavity. Measuring such higher-order correlations allows one to discriminate output fields even in case, when the $g^{(2)}(0)$ function value is equal. For example, the Fock state higher-order correlation functions read $g^{(n)}_{\rm Fock}(0) = N!/[N^n(N-n)!]$ for $n < N = \langle a^\dagger a\rangle$ and therefore $g^{(n)}_{\rm Fock}(0) > g^{(n+1)}_{\rm Fock}(0)$ in contrast to a coherent distribution, which holds $g^{(n)}_{\rm coh}(0) = g^{(n+1)}_{\rm coh}(0) = 1$. For a thermal light field with $\bar{n}$ mean photon number, the unnormalized higher-order correlation functions read $\langle a^{\dagger n} a^n\rangle = n!(\bar{n})^n$ and are calculated from $p_n = (\bar{n})^n/(1+\bar{n})^{n+1}$. For the correlation function it holds then that $g^{(n)}_{\rm therm}(0) < g^{(n+1)}_{\rm therm}(0) = (n+1)!$. We take these three limiting cases to visualize our quantum cascade driving setup.

In Fig. 3, we plot the higher-order correlation functions for the source cavity (red, solid) and the target cavity with one (blue, dashed dotted) and two (green, dashed) TLSs. To illustrate regimes, we shaded the areas that distinguish between superthermal and subthermal fields, and super- and sub-Fock states. The Fock state limits are taken so that the number of Fock photons equals the order of the correlation function $N = n$. The correlations of the source $g_s^{(n)}(0)$ and target system $g_t^{(n)}(0)$ are shown for $\Gamma_s^P = 0.1\ {\rm ps}^{-1} = g$. The output field of the source shows a monotonic behavior, i.e., $g_s^{(n)} > g^{(m)}$ for all $n < m < 10$. That is, comparing to the shaded area, very characteristic for a nonclassical output field. For one TLS in the target cavity, we also see a monotonic behavior, but this time

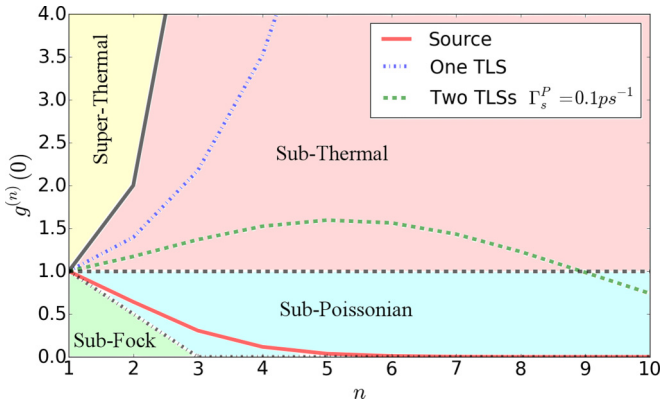

FIG. 3. Correlation functions in the steady state, when the pump strength is equal to the cavity coupling ($\Gamma_s^P = g$) for source (red, solid) and target with two TLSs (green, dashed) and a single TLS (blue, dashed dotted). The solid, dashed, and dash-dotted gray lines represent thermal, coherent, and pure quantum light (for example, the two photon Fock state). The source is antibunched and in the sub-Poissonian regime for all orders in the correlation function. The target with a single TLS exhibits thermal light. However, the target cavity when containing two TLSs shows a transitional behavior, where it starts out in the subthermal regime but goes to the sub-Poissonian regime for higher orders.

with $g_s^{(n)} < g^{(m)}$ for all $n < m < 10$. In contrast, the output field of the target with two TLSs does not exhibit this kind of monotonic behavior; e.g., $g_t^{(2)}(0) < g_t^{(3)}$ but $g_t^{(2)}(0) > g_t^{(6)}$. Given this difference, it is clear that the target dynamics is not a simple image of the source; the differences cannot only be traced back to dissipative degradation from the source-target transfer. In the following, we will focus on the case of two TLSs because we find interesting photon probability distributions for this case, and also because the target system with one emitter does not show nonmonotonic behavior in the parameter regime in which we are interested. The quantum cascade coupling introduces its own remarkable behavior and prevents a straightforward imprinting of the source statistics on the target quantum statistics, i.e., the $g_t^{(n)}(0)$ distribution.

In Fig. 4, we investigate the higher-order correlation functions of the source $g_s^{(n)}(0)$ and target systems $g_t^{(n)}(0)$ for different incoherent pumping strengths of the source system Γ_s^P. Interestingly, the response of the target differs strongly from the source quantum statistics. The source system shows a monotonic behavior for all pumping strengths: $g_s^{(n)}(0) > g_s^{(m)}(0)$ for all $n < m \leqslant 10$. Furthermore, the quantum statistics approaches lower values and reaches small values for high orders. This behavior is expected, since the incoherent driving and the cooperativity [64] $C_s = g_s^2/(\Gamma_R \kappa_s)$ limits the achievable photon manifold; i.e., there is always a cutoff n_c with $p_{n_c} = 0$ and therefore the importance of higher-order correlations decreases: $g_s^{(n)}(0) \to 0$ for $(n - n_c) \to 0$.

In contrast, the target system reaches first a maximum for a certain m with $g_t^{(m)}(0) \geqslant g_t^{(n)}(0)$ for all n. This maximum shifts, as expected, for higher pumping strength towards larger m, since the maximum number of photons also shifts to larger values. After the maximum, the $g_t^{(n)}(0)$ distribution follows the trend of the source system towards lower values. This behavior is stable for a wide range of pumping strengths. Due to the presence of a cutoff in the source photon manifold n_c, the target quantum distributions will also, eventually, tend towards zero. However, the target system follows only for large n the source quantum statistics, always after passing a maximum. This maximum, however, can shift to very high orders in the correlations.

Furthermore, Fig. 4 shows a qualitative transition of the target system in the correlation functions. For low incoherent pump strengths, the curve is turning downwards. Then there is a transition towards the regime, where the curve turns upwards. We quantify this by the second-order central difference defined as

$$g^{(n)\prime\prime} = \frac{g^{(n+1)} - 2g^{(n)} + g^{(n-1)}}{(n+1-n)[n-(n-1)]}. \tag{15}$$

During the transition from coherent to thermal behavior, the nthorder correlation function will flip successively up. Here, we characterize this transition by the second-order difference at the $g^{(2)}$ function, which will first show the flip, so that the curve points here upwards. This is shown in Fig. 5, where we observe that the target system goes from a downwards to an upwards turning point. At the same time the source system shows a transition from an upwards to a downwards turning point. The curves cross at the coupling strength $g = 0.1$ ps^{-1}. Thus, even though it is not straightforwardly obvious how the source influences the target, we can illustrate the transition in

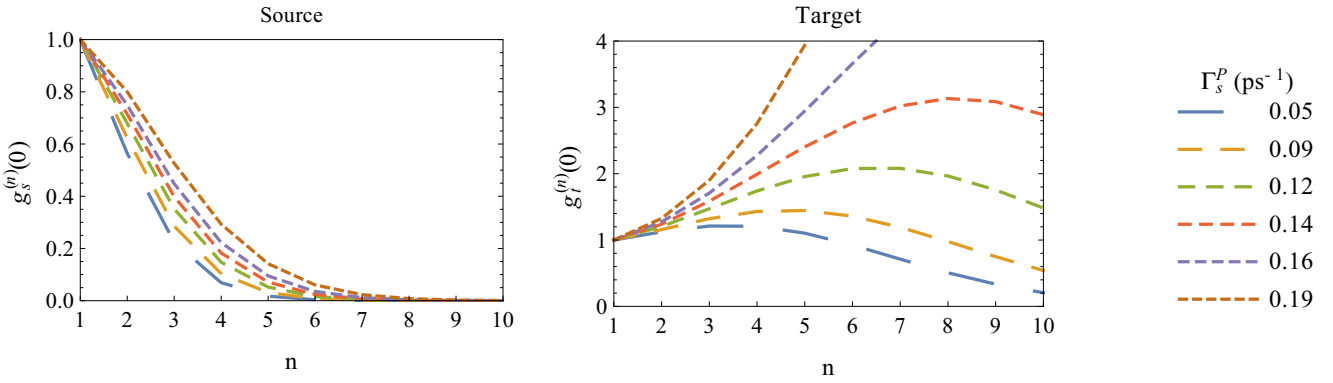

FIG. 4. Higher-order correlation functions of the source $g_s^{(n)}(0)$ and target system with two emitters $g_t^{(n)}(0)$ for different incoherent pumping strengths of the source system Γ_s^P. Remarkably, the target system exhibits a different behavior than the source system.

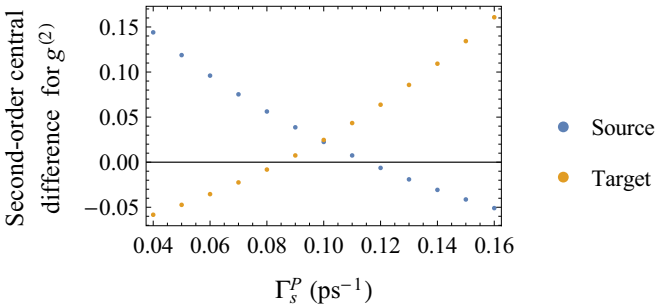

FIG. 5. The transition observed in the system illustrated by the second-order finite difference at the $g^{(2)}$ function. While the source correlations cross from an upwards to a downwards turning point, the target correlations exhibit the opposing behavior. The curves cross at the coupling strength $g = 0.1$ ps^{-1} common to source and target (with two emitters).

the target system by a corresponding transition in the source system

To explain the origin of our results, in the next section, we compare the quantum statistics of the target system with a coherent and incoherent drive. We will see that this maximum in the photon correlation is not readily produced with either coherent or incoherent driving. Thus, the cascaded setup allows one to create photon statistics not achievable with a reduced formulation.

V. PROPERTIES OF CASCADED DRIVING

To characterize the quantum cascade, we compare the resulting higher-order correlation with a system that is coherently or incoherently driven. To model this situation, we switch the coupling between the source and target systems off by setting $\kappa_s = 0$. The driving of the target system is now included for the coherent driving by displacing the target's photon operator according to $a_t^\dagger \to a_t^\dagger + \Gamma_t^P/g_t$, and for the incoherent driving case we switch the operators of the incoherent pumping from $\mathcal{D}[\sqrt{\Gamma_s^P}\sigma_s^+]\rho \to \mathcal{D}[\sqrt{\Gamma_t^P}\sigma_t^+]\rho$.

In Fig. 6, we compare the higher-order correlation functions for the case of coherent pumping (left panel) and incoherent pumping (right panel) of the target system. All parameter values are kept to allow comparison with the quantum cascaded case. Comparing the behavior of the correlation functions in the cascaded setup (cf. Fig. 4), with the incoherently and the coherently pump cases, we see a qualitatively different behavior. While the cascaded setup exhibits a maximum in the correlation functions, the incoherently driven one exhibits thermal behavior, increasing monotonically, and the coherently driven system exhibits close-to-coherent statistics. The form of the photon statistics for the cascaded system is distinctly different than for the other excitation scenarios studied in this manuscript. This is consistent with the findings in Ref. [30], where it is shown that, in principle, the target of a stationary cascaded system may access parts of the Hilbert space that would not be accessible by other means. Here, we illustrate this finding by showing a physical system realizing this possibility.

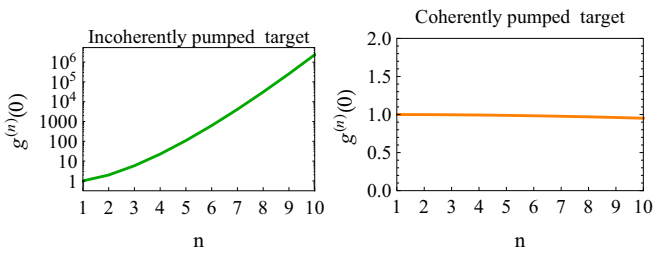

FIG. 6. Higher-order correlation functions of the target system with two emitters and without quantum source pumping $\kappa_t = \Gamma_s^P = 0$. Instead the target is directly pumped incoherently (left) and coherently (right) with $\Gamma_t^P = \sqrt{\gamma_t \kappa_s}$. Note the logarithmic scale for incoherent pumping, and the monotonic increase in contrast to the coherent driving induced maximum in the $g^{(n)}(0)$ distribution. The incoherent driving exhibits thermal statistics, while the coherent driving is close to coherent statistics for a wide range of pump parameters.

If we inspect the coupling terms, we can give some physical intuition for the observed result. The coherent driving creates excitation inside the emitters without destroying the coherences. Incoherent driving creates excitation, but, at the same time, destroys the coherence inside the system. With this is mind, we take a closer look at the derivation of the cascaded coupling.

The cascaded coupling is derived using an intermediate bath and thus constitutes a dissipative coupling and the coupling preserves some properties of the source statistics in certain regimes. This becomes clear from the master equation (12). If one exchanges $\sqrt{\gamma_t \kappa_s} \to -\sqrt{\gamma_t \kappa_s}$, the system dynamics and results remain unchanged, as it is the same with $H_{t/s} \to -H_{t/s}$. This explains the part of the dynamics that preserves the source photon statistics for low pump strengths. This is the case since for low pumping strengths this behavior is not expected from a dissipative coupling, as the standard Lindblad form is independent of a change in the sign. The term coupling the source and target system transfers excitations from the source cavity to the target emitters. For this, the source cavity needs a finite emission into the mediating bath.

However, the target emitters also need to have a finite decay in order to receive input from the source. With this, it also is subject to loss of excitation and destruction of coherence. This distinguishes the cascaded coupling from coherent and incoherent driving, as a loss of excitation is mandatory. For two TLSs the nonmonotonic behavior becomes more pronounced as the correlation is lowered more due to the stronger nonlinearity of the target with two TLSs [cf. Fig. 2]. Thus, the transitional behavior is visible more clearly for two TLSs and we use this case for illustration.

For weak incoherent pumping, quantum coherences can be built up and those quantum processes are mediated via $a_s^\dagger$ to the coherences of the target system σ_t^+. In this limit, for high pumping strengths, the system becomes thermal. However, the intermediate coupling regime shows the transition, allowing for peculiar distributions by only partially imprinting the source photon statistics on the target in the high-order correlation functions. The Fock distribution corresponding to the statistics in Fig. 3 is shown in Fig. 7. Here, we observe a very flat distribution exhibiting a similar probability for the first few photon number states (solid,blue). This deviates

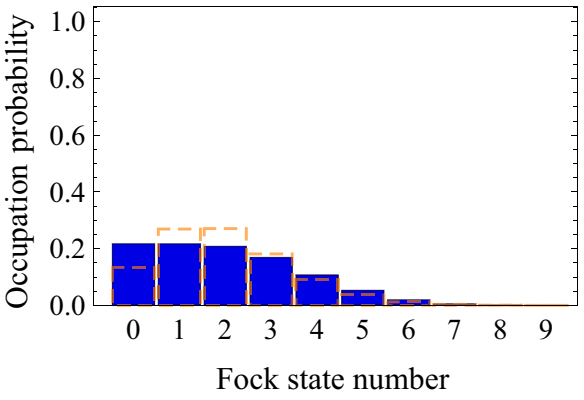

FIG. 7. Occupation probability of the Fock states for the target system with two emitters at $\Gamma_s^P = 0.1$ ps^{-1} corresponding to the photon statistics shown in Fig. 3 (solid, blue). Due to the cascaded coupling the photon number distribution is exceptionally flat. This illustrates the photon statistics that deviate from the prototypical cases. For reference (dashed, orange), the coherent distribution is shown.

from the coherent distribution (dashed,orange), which exhibits a maximum, and the thermal distribution, which decreases monotonically. With this, we can explain the accessibility of new photon statistics by the mixture of Hamiltonian and decoherent coupling processes, mediated by the cascaded setup.

VI. CONCLUSION AND OUTLOOK

We investigated a quantum cascaded system, in which an incoherently pumped source system drives a target system with its quantum output field. As observables, we focused on higher-order photon correlations $g^{(n)}(0)$. We find that the response of the target system differs strongly for different values of the incoherent pump parameter. For low values in comparison to the coupling constant of the target system $\Gamma_s^P < g_t$, the quantum statistics of the source system are imprinted on the target system. For larger values the target system's output field resembles an incoherently driven quantum system. However, in an intermediate regime, a mixture of coherent and incoherent processes due to the coupling mechanism occurs, leading to quantum statistics differing from the prototypical coherent and thermal shapes and giving rise to the possibility of producing flat photon distributions. For future work two promising directions for further study were already discussed before in the paper. On the one hand, expanding the systems to describe the emitter more realistically, e.g., by using a semiconductor model to describe quantum dots, is a way to establish the effect of more complex emitters on the output statistics [1]. On the other hand, considering a different type of bath may give some insights into how the transfer of photon statistics between systems may be facilitated. For most realizations, this requires a more careful consideration of the bath degrees of freedom. However, some special cases, such as a squeezed bath [65], may already be treated in the formalism presented in this work.

ACKNOWLEDGMENTS

S.C.A. thanks the DAAD foundation for the visiting research grants. N.L.N., A.K., and A.C. are grateful towards the Deutsche Forschungsgemeinschaft for support through SFB 910 "Control of self-organizing nonlinear systems" (project B1). N.L.N also acknowledges support through the School of Nanophotonics (Deutsche Forschungsgemeinschaft SFB 787).

[1] A. J. Shields, Nat. Photon. **1**, 215 (2007).
[2] N. Sim, M. F. Cheng, D. Bessarab, C. M. Jones, and L. A. Krivitsky, Phys. Rev. Lett. **109**, 113601 (2012).
[3] C. S. Munoz, E. del Valle, A. G. Tudela, K. Muller, S. Lichtmannecker, M. Kaniber, C. Tejedor, J. Finley, and F. P. Laussy, Nat. Photon. **8**, 550 (2014).
[4] P. Lodahl, S. Mahmoodian, S. Stobbe, A. Rauschenbeutel, P. Schneeweiss, J. Volz, H. Pichler, and P. Zoller, Nature (London) **541**, 473 (2017).
[5] S. Strauf and F. Jahnke, Laser Photon. Rev. **5**, 607 (2011).
[6] J. Kabuss, A. Carmele, M. Richter, and A. Knorr, Phys. Rev. B **84**, 125324 (2011).
[7] A. Gonzalez-Tudela, F. P. Laussy, C. Tejedor, M. J. Hartmann, and E. del Valle, New J. Phys. **15**, 033036 (2013).
[8] M. Peiris, K. Konthasinghe, and A. Muller, Phys. Rev. Lett. **118**, 030501 (2017).
[9] K. E. Dorfman, F. Schlawin, and S. Mukamel, Rev. Mod. Phys. **88**, 045008 (2016).
[10] M. Kira, S. W. Koch, R. P. Smith, A. E. Hunter, and S. T. Cundiff, Nat. Phys. **7**, 799 (2011).
[11] M. Kira and S. W. Koch, Phys. Rev. A **73**, 013813 (2006).
[12] M. Kira and S. Koch, Prog. Quantum Electron. **30**, 155 (2006).
[13] I. Aharonovich, D. Englund, and M. Toth, Nat. Photon. **10**, 631 (2016).
[14] V. A. Gaisler, Bull. Russ. Acad. Sci. Phys. **73**, 77 (2009).
[15] S. Buckley, K. Rivoire, and J. Vučković, Rep. Prog. Phys. **75**, 126503 (2012).
[16] H. J. Kimble, Nature (London) **453**, 1023 (2008).
[17] P. Zoller, T. Beth, D. Binosi, R. Blatt, H. Briegel, D. Bruss, T. Calarco, J. I. Cirac, D. Deutsch, J. Eisert, *et al.*, Eur. Phys. J. D **36**, 203 (2005).
[18] T. Jennewein, C. Simon, G. Weihs, H. Weinfurter, and A. Zeilinger, Phys. Rev. Lett. **84**, 4729 (2000).
[19] I. A. Walmsley, Science **348**, 525 (2015).
[20] R. Beach and S. R. Hartmann, Phys. Rev. Lett. **53**, 663 (1984).
[21] M. Strauß, M. Placke, S. Kreinberg, C. Schneider, M. Kamp, S. Höfling, J. Wolters, and S. Reitzenstein, Phys. Rev. B **93**, 241306 (2016).
[22] M. Aßmann and M. Bayer, Phys. Rev. A **84**, 053806 (2011).
[23] F. Jahnke, C. Gies, M. Aßmann, M. Bayer, H. Leymann, A. Foerster, J. Wiersig, C. Schneider, M. Kamp, and S. Höfling, Nat. commun. **7** 11540 (2016).

[24] T. Kazimierczuk, J. Schmutzler, M. Aßmann, C. Schneider, M. Kamp, S. Höfling, and M. Bayer, Phys. Rev. Lett. **115**, 027401 (2015).
[25] S. Schumacher, J. Förstner, A. Zrenner, M. Florian, C. Gies, P. Gartner, and F. Jahnke, Opt. Express **20**, 5335 (2012).
[26] A. Lochmann, E. Stock, O. Schulz, F. Hopfer, D. Bimberg, V. A. Haisler, A. I. Toropov, A. K. Bakarov, and A. K. Kalagin, Electron. Lett. **42**, 774 (2006).
[27] T. Heindel, A. Thoma, M. Helversen, M. Schmidt, A. Schlehahn, M. Gschrey, P. Schnauber, J. H. Schulze, A. Strittmatter, J. Beyer, S. Rodt, A. Carmele, A. Knorr, and S. Reitzenstein, Nat. Commun. **8**, 14870 (2017).
[28] S. Bounouar, M. Strauß, A. Carmele, P. Schnauber, A. Thoma, M. Gschrey, J.-H. Schulze, A. Strittmatter, S. Rodt, A. Knorr, and S. Reitzenstein, Phys. Rev. Lett. **118**, 233601 (2017).
[29] J. C. López Carreño, C. Sánchez Muñoz, D. Sanvitto, E. del Valle, and F. P. Laussy, Phys. Rev. Lett. **115**, 196402 (2015).
[30] J. C. López Carreño and F. P. Laussy, Phys. Rev. A **94**, 063825 (2016).
[31] M. Richter and S. Mukamel, Phys. Rev. A **82**, 013820 (2010).
[32] F. Troiani, Phys. Rev. B **90**, 245419 (2014).
[33] F. Schlawin and A. Buchleitner, arXiv:1510.06726.
[34] J. L. Hall, M. Zhu, and P. Buch, J. Opt. Soc. Am. B **6**, 2194 (1989).
[35] A. Carmele, A. Knorr, and M. Richter, Phys. Rev. B **79**, 035316 (2009).
[36] T. S. Theuerholz, A. Carmele, M. Richter, and A. Knorr, Phys. Rev. B **87**, 245313 (2013).
[37] C. W. Gardiner, Phys. Rev. Lett. **70**, 2269 (1993).
[38] H. J. Carmichael, Phys. Rev. Lett. **70**, 2273 (1993).
[39] P. Kochan and H. J. Carmichael, Phys. Rev. A **50**, 1700 (1994); C. W. Gardiner and A. S. Parkins, *ibid.* **50**, 1792 (1994); A. S. Parkins, *ibid.* **53**, 2893 (1996).
[40] J. C. López Carreño, C. Sánchez Muñoz, E. del Valle, and F. P. Laussy, Phys. Rev. A **94**, 063826 (2016).
[41] C. W. Gardiner and P. Zoller, *Quantum Noise*, 2nd ed. (Springer, Berlin, 2000).
[42] H. Carmichael, *An Open Systems Approach to Quantum Optics: Lectures Presented at the Université Libre de Bruxelles, October 28 to November 4, 1991*, Lecture Notes in Physics Monographs Vol. 18 (Springer, Berlin, 1993).
[43] Y. Lu, N. L. Naumann, J. Cerrillo, Q. Zhao, A. Knorr, and A. Carmele, Phys. Rev. A **95**, 063840 (2017).
[44] L. Lu, J. D. Joannopoulos, and M. Soljačić, Nat. Photonics **8**, 821 (2014).
[45] C. W. Gardiner and M. J. Collett, Phys. Rev. A **31**, 3761 (1985).
[46] H. Pichler and P. Zoller, Phys. Rev. Lett. **116**, 093601 (2016).
[47] I. M. Mirza and S. van Enk, Opt. Commun. **343**, 172 (2015); I. M. Mirza, S. J. van Enk, and H. J. Kimble, J. Opt. Soc. Am. B **30**, 2640 (2013).
[48] M. J. Collett and C. W. Gardiner, Phys. Rev. A **30**, 1386 (1984); C. W. Gardiner, Phys. Rev. Lett. **56**, 1917 (1986).
[49] M. Richter, A. Carmele, S. Butscher, N. Bücking, F. Milde, P. Kratzer, M. Scheffler, and A. Knorr, J. Appl. Phys. **105**, 122409 (2009).
[50] J. Cerrillo and J. Cao, Phys. Rev. Lett. **112**, 110401 (2014).
[51] J. Kabuss, A. Carmele, M. Richter, W. W. Chow, and A. Knorr, Phys. Status Solidi B **248**, 872 (2011).
[52] J. Prior, A. W. Chin, S. F. Huelga, and M. B. Plenio, Phys. Rev. Lett. **105**, 050404 (2010).
[53] H. P. Breuer and F. Petruccione, *The Theory of Open Quantum Systems* (Oxford University Press, Oxford, 2002).
[54] H. J. Carmichael, *Statistical Methods in Quantum Optics 1* (Springer, Berlin, 1999).
[55] E. del Valle and F. P. Laussy, Phys. Rev. Lett. **105**, 233601 (2010); P. Gartner, Phys. Rev. A **84**, 053804 (2011).
[56] R. M. Stevenson, R. J. Young, P. Atkinson, K. Cooper, D. A. Ritchie, and A. J. Shields, Nature (London) **439**, 179 (2006).
[57] Z. Yuan, B. E. Kardynal, R. M. Stevenson, A. J. Shields, C. J. Lobo, K. Cooper, N. S. Beattie, D. A. Ritchie, and M. Pepper, Science **295**, 102 (2002).
[58] F. Schulze, B. Lingnau, S. M. Hein, A. Carmele, E. Schöll, K. Lüdge, and A. Knorr, Phys. Rev. A **89**, 041801 (2014).
[59] A. Siegman, *Lasers* (University Science Books, Mill Valley, CA, 1986), Chap. 6.
[60] R. Loudon, *The Quantum Theory of Light* (Oxford University Press, Oxford, 2000).
[61] P. R. Rice and H. J. Carmichael, Phys. Rev. A **50**, 4318 (1994).
[62] S. Ritter, P. Gartner, C. Gies, and F. Jahnke, Opt. Express **18**, 9909 (2010).
[63] M. Aßmann, F. Veit, M. Bayer, M. van der Poel, and J. M. Hvam, Science **325**, 297 (2009).
[64] D. F. Walls and G. J. Milburn, *Quantum optics*, 2nd ed. (Springer Berlin, 2008).
[65] *Springer Handbook of Atomic, Molecular, and Optical Physics*, edited by G. W. F. Drake (Springer, Berlin, 2006), Chap. 78.